CHAPTER 8

Assessment of Microporosity

8.1. Introduction 219
8.2. Isotherm analysis 222
8.2.1. Empirical methods 222
8.2.2. Dubinin–Stoeckli methods 224
8.2.3. Nonane pre-adsorption 226
8.2.4. Generalized adsorption isotherm (GAI) 226
8.3. Microcalorimetric methods 227
8.3.1. Immersion microcalorimetry 227
Immersion of various dry samples in the same liquid 227
Immersion of dry samples in liquids of different molecular size 228
Immersion of samples partially pre-covered by vapour adsorption 229
8.3.2. Gas adsorption microcalorimetry 229
8.4. Modelling micropore filling: theory and simulation 230
8.4.1. Potential energy functions 230
8.4.2. Horvath–Kawazoe (HK) method 231
8.4.3. Computer simulation and density functional theory 233

8.1. Introduction

We recall that the filling of micropores (of width < 2 nm) takes place in the pre-capillary condensation range of a physisorption isotherm. If the pore width, w, is no greater than a few molecular diameters (i.e. in an ultramicropore), the pore filling occurs at a very low $p/p°$. This process, which we refer to as the 'primary micropore filling', is associated with enhanced adsorbent–adsorbate interactions and always involves some distortion of the sub-monolayer isotherm. Wider micropores (super-micropores) are filled by a co-operative process over a somewhat higher range of $p/p°$, which may extend into the multilayer region.

Recent theoretical, simulation and experimental studies of physisorption energetics and phase equilibria have helped to improve our understanding of the differences between these two mechanisms of micropore filling. It is now evident that there are six main variables which must be taken into account:

(a) the adsorbent solid structure;
(b) the surface composition;
(c) the pore width and shape;
(d) the polarizabilities and polarities of the interacting centres;

(e) the adsorptive molecular size and shape;
(f) the operational temperature.

In addition, we should keep in mind that the micropore filling capacity is dependent on both the available pore volume and the packing of the adsorbed molecules.

In this chapter, we introduce the currently most popular adsorption methods used for micropore size analysis: our aim is to outline in general terms the relative merits and limitations of these procedures. Their application is discussed more fully in later chapters in relation to the characterization of particular adsorbents.

As we have already seen, an ideal Type I isotherm has a long, almost horizontal plateau, which extends up to $p/p^\circ \longrightarrow 1$, as in Figure 8.1a. In this case, the micropore capacity, n_p(mic), is registered directly as the amount adsorbed at the plateau. Such well-defined Type I isotherms are given by large crystals of a molecular sieve zeolite.

Many porous adsorbents contain pores with a wide range of sizes which cross the micropore–mesopore boundary. Also, some microporous adsorbents are composed of very small agglomerated particles, which exhibit a significant external area. Such materials give composite isotherms with no distinctive plateau. The presence of mesopores can often be detected by the appearance of a hysteresis loop – as in Figure 8.1b.

A third possibility is a Type I isotherm with a short plateau, which terminates at $p/p^\circ < 1$. An upward deviation, as indicated in Figure 8.1c, occurs at high p/p° when the microporous adsorbent also contains some wide mesopores or narrow macropores. Since the wall area of such relatively wide pores is likely to be much smaller than the micropore area, the scale of multilayer development or mesopore filling may be quite small.

Many attempts have been made to obtain the micropore capacity by the analysis of composite isotherms. The calculation of the micropore volume, v_p(mic), from n_p(mic) is almost invariably based on the assumption that the adsorbate in the micropores has the same density as the adsorptive in the liquid state at the operational

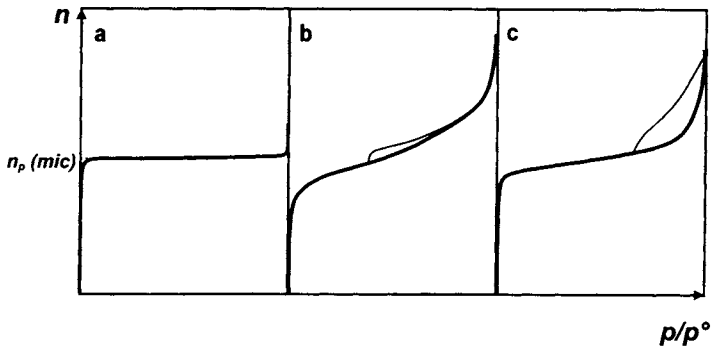

Figure 8.1. Nitrogen isotherms corresponding to adsorption: (a) in ultramicropores; (b) in wider micropores and on external surfaces; (c) in micropores and wide mesopores.

temperature. As we saw in Chapter 7, for the condensate in a mesoporous adsorbent this assumption (i.e. the Gurvich rule) appears to be justified. The situation is quite different, however, with a microporous material – particularly when the pore dimensions are in the ultramicropore range.

Studies of the packing of molecules in cylindrical and slit-shaped pores have revealed the importance of both the width and the shape of narrow pores (Carrott *et al.*, 1987; Balbuena and Gubbins, 1994). An indication of the effect of pore size on the packing density of spherical molecules is given in Figure 8.2. Here, the degree of packing in cylinders and slits is expressed as a percentage of the packing density in the corresponding close-packed state. Although this is an oversimplified picture since it does not allow for the adsorption forces, it does illustrate the difficulty of arriving at an unambiguous assessment of the accessible pore volume. Inspection of

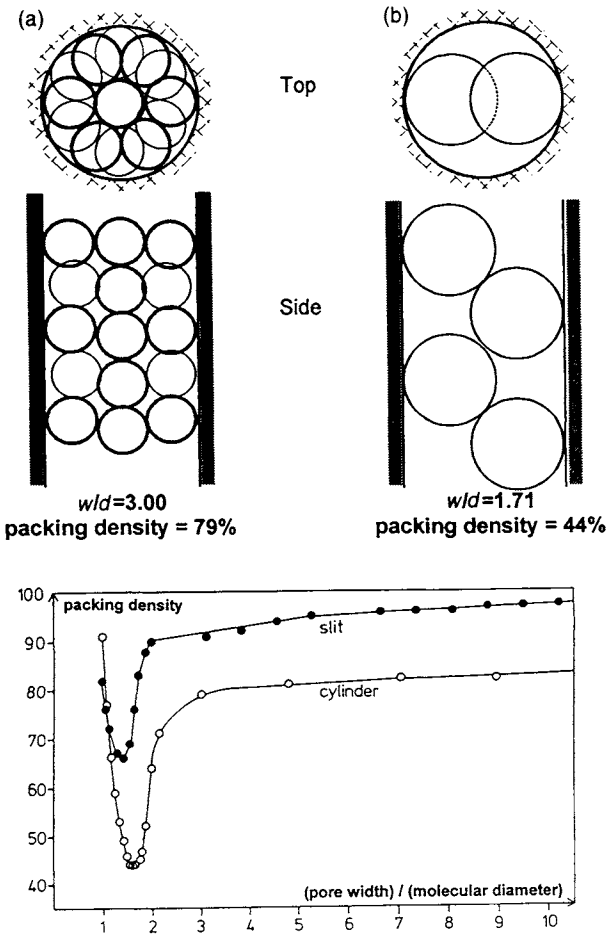

Figure 8.2. Packing of spherical molecules in narrow cylinders and slits.

Figure 8.2 reveals that the Gurvich rule is more likely be obeyed if $w/d > 4$. Of course, conformity to the Gurvich rule does not by itself guarantee that the packing densities are the same as in the bulk liquid.

The most striking feature of Figure 8.2 is the effect of the additional degree of freedom provided by a parallel-sided slit. Indeed, this difference in the packing density in slits and cylinders will be seen to be of great importance when we consider the adsorptive properties of molecular sieve carbons and certain zeolites.

In assessing the packing densities within narrow slits and cylinders, we have assumed that the same width is available for all molecules within a given slit or cylinder. This cannot be strictly true, however, since the effective pore width is to some extent dependent on the molecular interactions (Everett and Powl, 1976). Indeed, the adsorbate can be regarded as an inhomogeneous fluid with a density which varies from one point to another within a given pore.

Of course, one possible reason for an observed large departure from the Gurvich rule is as a direct result of molecular sieving: that is, the inability of larger adsorptive molecules to enter a certain range of narrow pores. Behaviour of this type is well documented for many zeolites and some activated carbons. Size exclusion measurements (gas adsorption or immersion calorimetry) provide an obvious way of determining the micropore size distribution (Gonzalez *et al.*, 1997; Lopez-Ramon *et al.*, 1997). Even when exclusion effects are small, or even absent, the use of molecules of different size is strongly recommended for the characterization of microporous adsorbents.

8.2. Isotherm Analysis

8.2.1. Empirical methods

Several early attempts were made to adapt the *t*-method for micropore analysis. In their original work, Lippens and de Boer (1965) had proposed that the total surface area of a porous solid was directly proportional to the slope of the initial linear section of a *t*-plot (see Section 6.3.2). In the MP (micropore)-method of Mikhail *et al.*, (1968), tangents to the *t*-plot were taken to represent the surface areas of different groups of micropores. The pore volume distribution was then determined for a given pore shape (e.g. parallel-sided slits). Although this apparently simple procedure attracted a good deal of interest, Dubinin (1970) and others (Gregg and Sing, 1976) pointed out that the MP method is fundamentally unsound. Since the isotherm is distorted as a result of primary micropore filling, it cannot be assumed that surface coverage or the effective molecular area are the same as on the open surface.

In principle, a *t*-plot can be used to assess the micropore capacity provided that the standard multilayer thickness curve has been determined on a non-porous reference material with a similar surface structure to that of the microporous sample. In our view, it is not safe to select a standard isotherm with the same BET C value (i.e. the procedure recommended by Brunauer (1970) and Lecloux and Pirard (1979)) since this does not allow for the fact that the sub-monolayer isotherm shape is dependent on both the surface chemistry and the micropore structure.

An important advantage of the α_s-method (see Section 6.3.3) is that it does not depend on any *a priori* assumptions concerning the mechanism of adsorption by the reference material and therefore its application is not restricted to nitrogen adsorption. For this reason it can be used to explore the various stages of micropore filling with a number of different adsorptives. As explained in Chapter 6, the standard isotherm is plotted in the reduced form, $(n/n_x)_s$ versus $p/p°$, the normalizing factor, n_X, being taken as the specific amount adsorbed at a pre-selected $p/p°$ (generally, it is convenient to take $p/p° = 0.4$).

To construct an α_S-plot for a given microporous adsorbent, the amount adsorbed, n, is plotted against the reduced standard adsorption, $\alpha_s = (n/n_X)_S$. Hypothetical α_S-plots for two different microporous adsorbents are shown in Figure 8.3. In the case of (a), there is no initial linear region since the isotherm is distorted at low $p/p°$ as a result of the enhanced adsorbent–adsorbate interactions in ultramicropores. However, the initial linear section of the α_S-plot in (b) corresponds to monolayer adsorption on the walls of supermicropores. Co-operative filling of the supermicropores occurs progressively over a range of higher $p/p°$ and in some cases is manifested by an upward deviation of the α_S-plot.

Once the micropores have been filled, both plots in Figure 8.3 become linear, provided that capillary condensation is absent (or only detectable at high $p/p°$). The low slope signifies that multilayer adsorption has occurred on a relatively small external surface. Back-extrapolation of the linear multilayer section gives the specific micropore capacity, n_p(mic), as the intercept on the n axis.

As already noted, the effective micropore volume, v_p(mic) is

$$v_p(\text{mic}) = n_p(\text{mic}) \times M/\rho \tag{8.1}$$

where M is the molar mass of the adsorptive and ρ is the average absolute density of the adsorbate, which is generally assumed to be the same as the absolute density of the liquid adsorptive.

The α_s-method has been used by a number of investigators to study the various stages of micropore filling (Fernandez-Colinas *et al.*, 1989; Carrott *et al.*, 1989; Kenny *et al.*, 1993; Kaneko, 1996). For example, high-resolution nitrogen measurements have

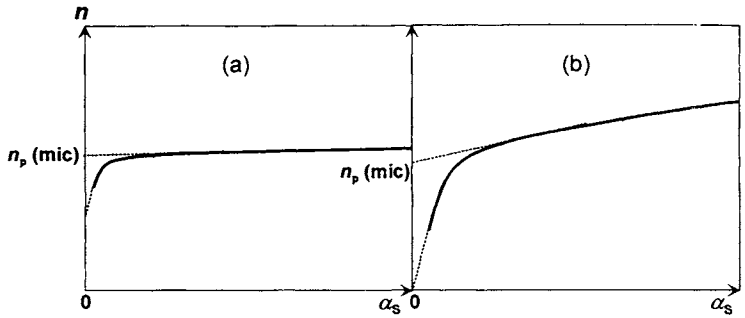

Figure 8.3. Hypothetical α_S plots for a sample with ultramicropores (a) and for a sample with only wider micropores or 'supermicropores' (b).

confirmed the differences in the adsorptive behaviour of ultramicroporous and supermicroporous carbons. Also, by constructing the α_S-plots for probe molecules of different size, one can study the effect of changing the ratio of pore width/molecular size, w/d, on the mechanism of pore filling (Carrott *et al.*, 1987, 1988). In this manner it is possible to gain a semi-quantitative estimate of the pore size distribution. This approach as applied to the characterization of activated carbons is illustrated in Chapter 9.

8.2.2. Dubinin–Stoeckli methods

The Dubinin–Radushkevich (DR) equation, which in Chapter 4 was given as Equation (4.43), can also be expressed in the form

$$\log_{10}(\boldsymbol{n}) = \log_{10}(\boldsymbol{n}_p(\text{mic})) - D\log^2_{10}(p°/p) \qquad (8.2)$$

where D is an empirical constant – as defined in Equation (4.44). Thus, according to the DR theory, a plot of $\log_{10}(\boldsymbol{n})$ against $\log^2_{10}(p°/p)$ should be linear with slope D and intercept $\log_{10}(\boldsymbol{n}_p(\text{mic}))$. As before, Equation (8.1) is used to obtain $v_p(\text{mic})$ from $\boldsymbol{n}_p(\text{mic})$.

Various DR plots for activated carbons are given in Chapter 9. For our present purpose, the two hypothetical examples in Figure 8.4 will suffice to illustrate some important features.

As a general rule, an ultramicroporous carbon gives a linear DR plot over a wide range of $p/p°$ (see Figure 8.4a) provided that the isotherm is reversible (i.e. there is no low-pressure hysteresis). Generally, any significant adsorption in wider pores or on an external surface leads to a departure from linearity (see Figure 8.4b). On the

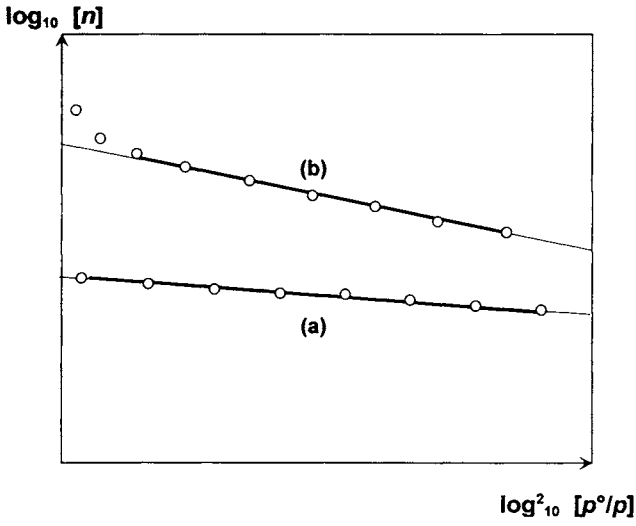

Figure 8.4. Hypothetical DR plots for a sample with only ultramicropores (a) and for a sample also including wider pores (b).

other hand, some DR plots on non-porous or mesoporous solids do exhibit limited ranges of linearity. In fact, it was this behaviour which led Kaganer (1959) to propose an analogous form of Equation (8.2) in which v_m(mic) is replaced by $\boldsymbol{n}_m$, the monolayer capacity.

It is apparent that any limited range of linearity of a simple DR plot cannot be used to give a reliable evaluation of the pore size distribution. In order to describe a bimodal micropore size distribution, Dubinin (1975) applied a two-term equation, which we may write in the form

$$\boldsymbol{n} = \boldsymbol{n}_{p,1} \exp[-(A/E_1)^2] + \boldsymbol{n}_{p,2} \exp[-(A/E_2)^2] \tag{8.3}$$

where $\boldsymbol{n}_{p,1}$ and $\boldsymbol{n}_{p,2}$ are the micropore capacities of the two groups of pores and E_1 and E_2 are the corresponding characteristic energies.

Of course, the application of Equation (8.3) is based on the assumption that there are two separate ranges of pore size. This led Dubinin (1975) to refer to the group of wider pores as the 'supermicropores', the width of which was considered to be *c.* 1.5 nm. In principle, Equation (8.3) could be extended to include a much larger number of different groups of pores, but in practice the resulting multi-term summations become intractable.

An important advance in the application of the DR equation to heterogeneous micropore structures was made by Stoeckli. By assuming a Gaussian distribution, Stoeckli and co-workers attempted to allow for a continuous distribution of pore size by replacing the summation of the individual DR contributions by integration (Stoeckli, 1977; Stoeckli *et al.*, 1979) (see Chapter 4). The integral transform was then solved by the use of a mathematical device equivalent to an 'error function' to give an exponential relation between the micropore size distribution and the Gaussian half-width, Δ. In other words, Δ was taken to be a measure of the dispersion of B around a mean value of B_0 in Equation (4.47).

To explain the significance of the various terms adopted by Dubinin and Stoeckli, it is convenient to write the Dubinin–Astakov equation – Equation (4.45) – in the form

$$\boldsymbol{n} = \boldsymbol{n}_p \exp[-(A/\beta E_0)^N] \tag{8.4}$$

where β and N are as defined in Chapter 4 and E in Equation (4.45) is replaced by βE_0. On the basis of a limited amount of experimental evidence, an inverse relation was proposed (Dubinin, 1979) between E_0 and the pore width, w:

$$w = K/E_0 \tag{8.5}$$

where K is an empirical constant, which was reported to be ≈ 17.5 nm kJ mol^{-1} for a series of activated carbons (see Bansal *et al.*, 1988). However, it was concluded that active carbons with characteristic E_0 values < 20–22 kJ mol^{-1} were likely to be heterogeneous. It appeared that the micropore size became smaller and the distribution also more homogeneous with increase in N over the range 1.5 to 3.0. The extreme value of $N = 3$ was found with a carbon molecular sieve, which had a particularly narrow distribution of pore size (Dubinin and Stoeckli, 1980).

The mathematical elegance of the Dubinin–Stoeckli approach is impressive, but it remains to be seen whether the basic DR equation is strictly applicable to a narrow

group of micropores of any size. It is noteworthy that the method appears to be most successful when applied to a relatively narrow range of ultramicropores in molecular sieve carbons, i.e. when only primary micropore filling is involved (Martin-Martinez *et al.*, 1986). Although the DA equation can be applied to physisorption isotherms on molecular sieve zeolites, the results are much more difficult to interpret. This is an indication that consideration must be given to both the pore structure and the surface chemistry.

8.2.3. Nonane pre-adsorption

A novel method for the evaluation of microporosity was introduced by Gregg and Langford (1969). The aim was to fill the micropores of an adsorbent with *n*-nonane, whilst leaving the wider pores and open surface still available for the adsorption of nitrogen at 77 K. Nonane was chosen as the pre-adsorptive because of its relatively large physisorption energy, which in turn results in a high energy barrier (i.e. activation energy) for desorption. As a consequence, elevated temperatures are required to remove the nonane molecules from the narrow pores at a measurable rate. Moreover, the long-chain molecules of *n*-nonane are able to enter narrow micropores of width as low as 0.4 nm, which is not the case with more bulky hydrocarbon molecules.

The following experimental procedure was used by Gregg and Langford. The outgassed adsorbent was first exposed to *n*-nonane vapour at 77 K, re-outgassed at room temperature and the first nitrogen isotherm determined at 77 K. The sample was then outgassed at a number of increasingly higher temperatures and nitrogen isotherms successively determined after each stage of outgassing until the nonane had been completely removed.

The first material to be studied in this way was an activated sample of carbon black. It was found that prolonged outgassing at a temperature of 350°C was required to achieve complete removal of the pre-adsorbed nonane. All the intermediate nitrogen isotherms were found to be parallel in the multilayer range and the vertical separation between the isotherms obtained after outgassing at 20° and 350°C provided a satisfactory measure of the micropore capacity. Convincing evidence was also obtained that the nonane was removed only from the external surface at 20°C.

Some more recent investigations of the pre-adsorption method have shown, however, that the results are not always so easy to interpret (Martin-Martinez *et al.*, 1986; Carrott *et al.*, 1989). As would be expected, the nonane molecules are more strongly trapped in ultramicropores than in supermicropores. However, since many microporous adsorbents have complex networks of pores of different size, the retention of the nonane molecules in narrow pores also leads to blocking of some wider pores.

8.2.4. Generalized adsorption isotherm (GAI)

A generalized expression for the adsorption isotherm given by a porous solid can be written in the integral form

$$n(\mathrm{p}) = \int n'(p, w)\mathrm{f}(w)\,\mathrm{d}w \tag{8.6}$$

where $n(p)$ is the total amount adsorbed at pressure p, $n'(p,w)$ represents a single-pore isotherm and $f(w)$ is a function of the pore size distribution. It is apparent that Equation (8.6) is equivalent to Equation (4.52), which is not explicitly related to the pore size distribution.

It follows that the derivation of a meaningful pore size distribution from an experimental isotherm is dependent on the availability of the appropriate single-pore isotherm data on a series of adsorbents of controlled pore size and shape (McEnaney and Mays, 1991). In practice, this requirement poses a serious problem with microporous adsorbents. As we have seen, it is unlikely that the same mathematical form of isotherm can hold for the complete range of filling of micropores of different size. The recent attempts to overcome this difficulty are discussed in the following sections.

8.3. Microcalorimetric Methods

Because of the appreciable enhancement of the adsorption potential in micropores of a few molecular diameters in width (see Section 1.7 and Figure 1.6), microcalorimetry can provide a useful means of assessing microporosity. The available experimental procedures are outlined in the following sections.

8.3.1. Immersion microcalorimetry

Immersion of various dry samples in the same liquid

For this approach, the liquid is usually selected to fill the micropores as completely as possible. The most popular liquids are water, methanol, benzene, cyclohexane and *n*-hexane; the choice depends on the expected polarity of the surface and shape of the micropores (cylindrical, slit-shaped, etc.).

The first stage is usually a simple comparison of the specific energies of immersion. In the absence of a relatively large external surface area, the energies are controlled by the nature of the microporous network (see for instance Stoeckli and Ballerini, 1991, or Rodriguez-Reinoso *et al.*, 1997).

For a more detailed evaluation of the microporosity, one must be able to interpret the energy of immersion data. At present, there are two procedures favoured by different investigators.

The first procedure is based on the Dubinin–Stoeckli principles of volume filling (see Section 4.4.4). The energy of immersion $\Delta_{imm}U$ is related to the *micropore volume* $W_0(d)$ and the 'characteristic energy' E_0 for a given micropore size and immersion liquid (Bansal *et al.*, 1988) by the expression:

$$\frac{\Delta_{imm}U}{m_s} = [-\beta E_0 W_0(d)(1 + \alpha T)\sqrt{\Pi}/2V_m^l] + u^i a(\text{ext}) \qquad (8.7)$$

where m_s is the mass of adsorbent, d is the molecular diameter, V_m^l is the molar volume of the liquid, u^i is the energy of immersion of 1 m^2 of external surface area

a(ext), β is a scaling factor and α is the coefficient of thermal expansion of the liquid. Provided the external surface area is negligible, the energy of immersion appears to provide an approximate comparative assessment of the microporous volume $W_0(d)$ accessible to the immersion liquid. However, this only holds if the characteristic energy, E_0, remains the same for all samples or if allowance can be made for the likely variation in E_0. Generally, this poses a serious problem.

The second procedure directly relates the energy of immersion $\Delta_{imm}U$ to the *micropore surface area* a(mic), as described in Section 6.5.2. As we saw, very simply:

$$\Delta_{imm}U = u_i a(\text{mic}) + u_i a(\text{ext}) \tag{8.8}$$

In spite of their great difference in complexity, Equations (8.7) and (8.8) are at least mutually consistent: since E is an inverse function of the pore width w, EW_0 may be approximately proportional to a(mic).

Immersion of dry samples in liquids of different molecular size

This method is designed to take advantage of molecular sieving. The basic data are simply in the form of a curve of the specific energy of immersion versus the molecular size of the immersion liquid. This provides immediate information on the micropore size distribution. For room-temperature experiments one can use the liquids listed in Table 8.1, which are well suited for the study of carbons. Because of the various ways of expressing the 'critical dimension' of a molecular probe or its 'molecular size', one must be careful to use a consistent set of data (hence the two separate lists in Table 8.1). Again, one can process the microcalorimetric data to compare either the micropore volumes accessible to the various molecules (see Stoeckli *et al.*, 1996), or the micropore surface areas, as illustrated in Figure 8.5.

A particular advantage of using immersion microcalorimetry for the study of ultramicroporous materials is that the molecular entry into very fine pores takes place much more rapidly from the liquid phase than from a gas. There are two reasons for this difference: gaseous diffusion may be slow (thermally activated) – especially at 77 K – and the higher liquid density also favours a more rapid molecular penetration.

Table 8.1 Immersion liquids used to probe micropore size

Liquid	Critical dimension[a] (nm)	Liquid	Molecular size[b] (nm)
Dichloromethane	0.33	Benzene	0.37
Benzene	0.41	Methanol	0.43
Cyclohexane	0.54	Isopropanol	0.47
Carbon tetrachloride	0.63	Cyclohexane	0.48
1,5,9-Cyclododecatriene	0.76	ter-Butanol	0.6
Tri 2,4-xylylphosphate	1.5	α-Pinene	0.7

[a] After Stoeckli (1993)
[b] After Denoyel *et al.*, (1993)

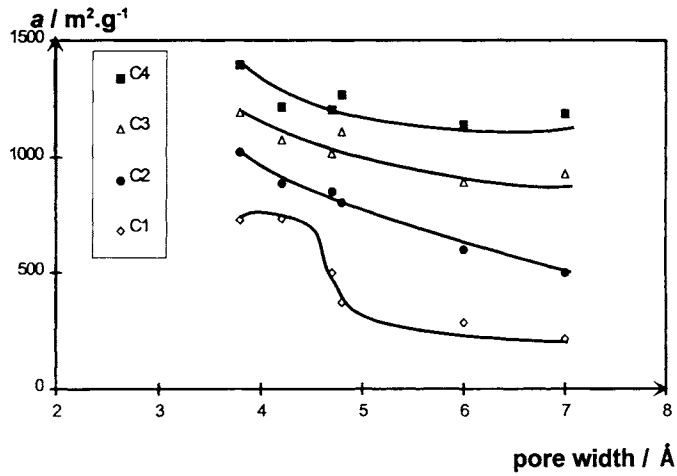

Figure 8.5. Accessible surface area versus pore width, from immersion microcalorimetry in the liquids listed in Table 8.1 (right-hand side) for a set of charcoals (activation increasing from C1 to C4) (Denoyel *et al.*, 1993).

Immersion of samples partially pre-covered by vapour adsorption

This is an indirect way of assessing the energetics of gas adsorption in micropores. The pre-adsorbed vapour can be that of the immersion liquid or it can be another adsorptive: for instance, to study the water filling mechanism in microporous carbons, Stoeckli and Huguenin (1992) devised an experiment with water pre-adsorption prior to immersion calorimetry (in water or in benzene).

8.3.2. Gas adsorption microcalorimetry

The enhancement of the potential energy in micropores can be directly assessed by microcalorimetric measurements of $\Delta_{ads} u$. Moreover, a comparison between N_2 and Ar adsorption allows one to distinguish between the enhancement due to the confinement in micropores and that due to specific adsorbent–adsorbate interactions. Both effects are manifested in the low-pressure range of the nitrogen isotherm, but the specific interactions are virtually absent with argon.

An important feature of gas adsorption microcalorimetry for the study of microporosity is that its highest sensitivity is in the low-pressure region (say, $p/p° < 0.05$), which is precisely the region of micropore filling and where the adsorption isotherm measurement often lacks accuracy. It follows that it is usually advisable to plot $\Delta_{ads} u$ versus n rather than versus $p/p°$. It is then possible to distinguish various types of micropores from the value of $\Delta_{ads} u$ and to obtain information on their effective volumes. This is illustrated by the microcalorimetric curves of Figure 9.14, obtained for nitrogen and argon adsorption on two activated carbons. In this manner, microcalorimetry is an independent way of checking the analysis of the isotherm. Values of $\Delta_{ads} u$ can be meaningful. For instance, with molecular sieve carbons, the

initial values of $\Delta_{ads}\dot{u}$ for nitrogen and argon are *c.* two-fold higher than those obtained on non-porous carbon black: this is the maximum enhancement predicted for the adsorption in slit-shaped micropores (Everett and Powl, 1976).

8.4. Modelling Micropore Filling: Theory and Simulation

8.4.1. Potential energy functions

Successful computer modelling of physisorption is dependent, *inter alia*, on the validity of the solid–fluid and fluid–fluid potential functions (Cracknell *et al.*, 1995). A rigorous description of the attractive and repulsive components is complex (see Nicholson, 1997); however, as was indicated in Chapter 1, the pairwise interaction between a single adsorbate atom and a solid atom is still usually expressed in the form of the 12-6 Lennard-Jones potential. For our present purpose, we may write

$$\varepsilon(r) = 4\,\varepsilon_{gs}[(\sigma/r)^{12} - (\sigma/r)^{6}] \tag{8.9}$$

where r is the distance between the centres of the two atoms, ε_{gs} is the depth of the potential energy well and here σ is the distance at which $\varepsilon(r) = 0$ (σ can also be regarded as the effective mean atomic diameter). According to the Lorentz combining rules, $\varepsilon_{gs} = (\varepsilon_g \times \varepsilon_s)^{1/2}$ and $\sigma = (\sigma_g + \sigma_s)/2$, where the subscripts g and s represent the gas and solid phases, respectively.

It was pointed out in Chapter 1 that it is usually assumed that the overall interaction energy between an adsorbate molecule and the adsorbent is given by the summation of the pairwise interactions. Furthermore, if the assemblage of discrete force centres in the solid can be treated as a continuum, the summation can be replaced by integration (Hill, 1952). In this case, the non-specific Lennard-Jones interaction energy between a single molecule and a semi-infinite slab of solid takes the 9-3 form (Steele, 1974):

$$\phi_{gs}(z) = 0.667\pi\rho\sigma^3\varepsilon_{gs}[0.133(\sigma/z)^9 - (\sigma/z)^3] \tag{8.10}$$

where ρ is the density of force centres in the adsorbent.

However, if the adsorbate–adsorbent interactions are confined to a single solid lattice plane, integration over the two dimensions of the solid gives a 10-4 potential function in place of Equation (8.10).

Everett and Powl (1976) applied both the 9-3 and the 10-4 expressions in their theoretical treatment of potential energy profiles for the adsorption of small molecules in slit-like and cylindrical micropores. As one would expect, the two corresponding potential energy curves were of a similar shape, but the differences between them became greater as the pore size was reduced. Strictly, the replacement of the summation by integration is dependent on the distance between the molecule and the surface plane, becoming more accurate as the distance is increased (Steele, 1974).

For the important case of the adsorption of a small molecule on a slab of graphite, Steele (1973) proposed a 10-4-3 potential:

$$\phi_{gs}(z) = 2\pi\rho\varepsilon_{gs}\sigma^2\Delta\{0.4(\sigma/z)^{10} - (\sigma/z)^4 - \sigma^4/[3\Delta(0.61\Delta + z)^3]\} \tag{8.11}$$

where z is the distance from the graphite surface, Δ is the distance between the graphite layers (0.335 nm) and ρ is the number of carbon atoms per unit volume (114 nm^{-3}). The derivation of this 10-4-3 potential function involved integration over the basal plane and summation over the successive layers. The 10- and 4- terms, therefore, represent the repulsive and attractive interactions with the basal plane, while the 3- term takes care of the summation over the remaining layers. This form of potential function has been favoured in recent computer simulation studies of the adsorption of molecules by porous carbons (Nicholson, 1996, 1997).

If the micropores can be pictured as uniform slits of width H within a graphitic structure, we have

$$\phi(z)_{pore} = \phi_{gs}(z) + \phi_{gs}(H - z) \tag{8.12}$$

where $\phi(z)_{pore}$ now represents the interaction of an adsorbate molecule with the two opposite walls of the slit. As we shall see later, H is the distance between the centres of the carbon atoms and must not be confused with the effective pore width, w.

The composition and size of the adsorbate molecule must be taken into account in the application of Equations (8.11) and (8.12). The nitrogen molecule is sufficiently small to be treated either as a single spherical interacting centre (Walton and Quirke, 1989) or alternatively as a diatomic species in which each atom is regarded as an interacting centre (Nicholson, 1996). For methane adsorbed on graphite, the continuum solid approximation appears to give satisfactory results at temperatures as low as 80 K (Cracknell *et al.*, 1995). In this case, the diameter of the molecule (0.381 nm) is large in comparison with the C—C spacing (0.142 nm) in the basal plane: the molecule therefore appears to move parallel to the surface at constant z.

8.4.2. Horvath–Kawazoe (HK) method

A novel method for determining the micropore size distribution was introduced by Horvath and Kawazoe in 1983. In its original form, the HK analysis was applied to nitrogen isotherms determined on molecular sieve carbons, the assumption being made that these adsorbents contained slit-shaped graphitic pores. More recently, the HK treatment has been extended to argon and nitrogen adsorption in cylindrical and spherical pores of zeolites and aluminophosphates (Venero and Chiou, 1988; Davis *et al.*, 1989; Saito and Foley, 1991; Cheng and Yang, 1995; Horvath and Suzuki, 1997).

The HK method is based on the general idea that the relative pressure required for the filling of micropores of a given size and shape is directly related to the adsorbent –adsorbate interaction energy. As in the FHH theory (see Section 4.2.5), the assumption is made that the entropy contribution to the free energy of adsorption is small in comparison with the large change of internal energy, which is itself largely dependent on the depth of the potential energy well. Expressed in another way, it is assumed that the molar entropy of the adsorbed phase is not very sensitive to a change in the pore dimensions.

By combining a simple 10-4 potential function and Equation (8.12), we have

$$\phi(z)_{\text{pore}} = k\int\left[\left(\frac{\sigma}{z}\right)^{10} - \left(\frac{\sigma}{z}\right)^{4} + \left(\frac{\sigma}{H-z}\right)^{10} - \left(\frac{\sigma}{H-z}\right)^{4}\right] \tag{8.13}$$

where z, σ and H are all as previously defined, and k is a constant for a given gas–solid system and temperature.

Equation (8.13) gives the potential at the distance z from each surface plane in the graphitic slit of width H. The average potential, ϕ_{pore}, in a given pore is obtained by integration across the effective pore width. In this manner, it is possible to evaluate the required relative pressure, $(p/p^\circ)_{\text{pore}}$, since it is assumed that

$$RT\ln(p/p^\circ)_{\text{pore}} = \text{f}[\phi(z)_{\text{pore}}] \tag{8.14}$$

By making use of the Kirkwood–Müller equation and substituting the available experimental data for the physical properties of nitrogen and carbon, Horvath and Kawazoe (1983) arrived at the following equation for the adsorption of nitrogen by molecular sieve carbons at 77 K:

$$\ln(p/p^\circ) = \frac{61.23}{(H-0.64)}\left[\frac{1.895\times10^{-3}}{(H-0.32)^3} - \frac{2.709\times10^{-7}}{(H-0.32)^9} - 0.05014\right] \tag{8.15}$$

Here, H is expressed in nm.

A few representative values of $(p/p^\circ)_{\text{pore}}$ obtained by the application of Equation (8.15) are given in Table 8.2. Although the HK method is based on questionable principles and is now overshadowed by the application of density functional theory, it merits recognition as the first stage in the development of a unified theoretical treatment of micropore filling.

Although the estimated values of $(p/p^\circ)_{\text{pore}}$ in Table 8.2 are unlikely to agree exactly with the equivalent experimental values, the predicted range is of interest. Thus, the filling of ultramicropores is expected to occur at very low relative pressures. In fact, the recent high-resolution adsorption studies of Conner (1997) and Maglara *et al.* (1997) have revealed that to investigate the first stages of micropore filling, it is necessary to work at $p/p^\circ < 10^{-5}$.

Table 8.2 HK predicted values of p/p° of N_2 required to fill carbon slit-shaped pores

Effective pore width w (nm)	$(p/p^\circ)_{\text{pore}}$
0.4	1.46×10^{-7}
0.5	1.05×10^{-5}
0.6	1.54×10^{-4}
0.8	2.95×10^{-3}
1.5	7.59×10^{-2}

8.4.3. Computer simulation and density functional theory

As indicated in Chapter 1, there is now considerable interest in the application of computer simulation (e.g. GCMC) and density functional theory (DFT) to physisorption in model pore structures. It is already possible to predict the behaviour of some simple fluids in model micropores of well-defined size and shape and further progress is to be expected within the next few years.

We have seen that the earlier methods of micropore analysis were either essentially empirical or based on questionable assumptions. In contrast, molecular simulation and DFT offer the prospect of a more rigorous treatment since they are based on the fundamental principles of statistical mechanics. However, it must be kept in mind that to solve the statistical mechanical Hamiltonian, it is necessary to know the exact position of the force centres in the solid structure and also the potential functions which govern the solid–fluid and fluid–fluid interactions. In view of the complexity of most porous adsorbents, it is not surprising that so far most attention has been given to the adsorption of small, spherical molecules in pores of uniform geometry –particularly cylindrical or slit-shaped pores (Steele and Bojan, 1997).

Because of its diatomic nature and permanent quadrupole moment, the physisorption of nitrogen at 77 K presents special problems. The application of DFT is facilitated if the molecules are assumed to be spherical, which was the approach originally adopted by Seaton *et al.* (1989) and also by Lastoskie *et al.* (1993). The analytical procedures already outlined in Chapter 7 (Section 7.6) do not depend on the meniscus curvature and are in principle applicable to both capillary condensation and micropore filling. The non-local version of the mean field theory (NLDFT), which was used by Lastoskie, gave excellent agreement with computer simulation when applied to the carbon slit pore model. However, as pointed out earlier, these computational procedures are not entirely independent since they involve the same model parameters.

With the aid of NLDFT, Lastoskie *et al.* (see Gubbins, 1997) have generated the 'individual pore isotherms' for nitrogen adsorption at 77 K for a wide range of slit-shaped pores. Wider pores (e.g. of $H/\sigma \approx 4$) were found to give Type IV isotherms: in this case the pore filling riser appeared to correspond to capillary condensation. At a smaller pore width a transition from the discontinous capillary condensation in mesopores to continuous filling in supermicropores was observed. Other continuous–discontinuous transitions were also detected at smaller pore widths, the double minima of the solid–fluid potential coming together to form a single deep well at $H \approx 0.8$ nm. At $H \approx 0.69$ nm, the enhancement of the potential well depth appeared to be maximized to approximately double its original depth on the open surface. At a smaller pore width, the repulsive forces became increasingly important and at 0.6 nm the pore space became inaccessible to nitrogen.

By computing a series of model single-pore isotherms for nitrogen adsorption at 77 K, Seaton, Gubbins, Olivier, Quirke and their co-workers (see Gubbins, 1997; Olivier, 1995) have been able to make use of Equation (8.6) in order to determine the micropore size distribution. It is assumed that all the pores are of the same shape (i.e. slits or cylinders of semi-infinite length) and that the distribution,

f(w), can be mathematically described by a function such as the gamma or log-normal distribution.

In applying DFT or MC simulation for the determination of pore size distribution, most investigators have not allowed for pore blocking or any other form of diffusion control. However, in a very recent study by Lopez-Ramon *et al.* (1997) an attempt has been made to make use of percolation theory along with GCMC simulation to interpret the isotherms of CH_4, CF_4 and SF_6 given by a microporous carbon. Although still at an early stage of development, it is already evident that there are a number of advantages in using various adsorptives at different temperatures. In principle, it becomes possible to assess the internal consistency of the derived pore size distribution and expose any aberrations due to networking or molecular sieving.

Most simulation studies of nitrogen adsorption have been made at 77 K. A higher operational temperature is likely to have the advantage that the effects due to quadrupolar interaction will become less important as the kinetic energy is increased. In the work of Kaneko *et al.* (1994), GCMC simulation was used to study the adsorption of nitrogen in slit-shaped graphitic micropores at 303 K.

The comparison of the GCMC isotherms with experimental data has brought to light the uncertainties involved in defining the effective pore width (i.e. the experimental property). Since the effective width of the pore depends on the temperature of measurement and the size of the probe molecule, it is virtually impossible to give a single value for the internal volume of a micropore (Rowlinson, 1985). However, Kaneko *et al.* (1994) suggest that it is practicable to take $\phi(z) = 0$ as a basis for defining the limits of pore width.

The question of the location of the interacting centres in the adsorbate molecule was also examined by Nicholson (1996). It was concluded that the differences between the one-centre and two-centre models, which are significant for the high fractional filling of nitrogen of a narrow micropore, can be attributed to differences in molecular packing. Thus, in the absence of quadrupolar interactions, the two-centre molecules are amenable to higher packing densities than the hypothetical one-centre molecules.

References

Balbuena P.B. and Gubbins K.E. (1994) In: *Characterization of Porous Solids III* (J. Rouquerol, F. Rodriguez-Reinoso, K.S.W. Sing and K.K. Unger, eds) Elsevier, Amsterdam, p. 41.

Bansal R.C., Donnet J.B. and Stoeckli H.F. (1988) In: *Active Carbon*, Marcel Dekker, New York, p. 139.

Brunauer S. (1970) In: *Surface Area Determination* (D.H. Everett and R.H. Ottewill, eds) Butterworths, London, p. 63.

Carrott P.J.M. and Sing K.S.W. (1988) In: *Characterization of Porous Solids I* (K.K. Unger, J. Rouquerol, K.S.W. Sing and H. Kral, eds) Elsevier, Amsterdam, p. 77.

Carrott P.J.M., Roberts R.A. and Sing K.S.W. (1987) *Chem. Ind.* 855.

Carrott P.J.M., Roberts R.A. and Sing K.S.W. (1988) In: *Characterization of Porous Solids I* (K.K. Unger, J. Rouquerol, K.S.W. Sing and H. Kral, eds) Elsevier, Amsterdam, p. 89.

Carrott P.J.M., Drummond F.C., Kenny M.B., Roberts R.A. and Sing K.S.W. (1989) *Colloids and Surfaces*, **37**, 1.

Cheng L.S. and Yang R.T. (1995) *Adsorption* **1**, 187.

Conner W.C. (1997) In: *Physical Adsorption: Experiment, Theory and Applications* (J. Fraissard and W.C. Conner, eds) Kluwer, Dordrecht, p. 33.
Cracknell R.F., Gubbins K.E., Maddox M.W. and Nicholson D. (1995) *Accounts Chem Res.* **28**, 281.
Davis M.E., Montes C., Hathaway P.E., Arhancet J.P., Hasha D.L. and Garces J. E. (1989) *J. Am. Chem. Soc.* **111**, 3919.
Denoyel R., Fernandez-Colinas F., Grillet Y. and Rouquerol J. (1993) *Langmuir* **9**, p. 515.
Dubinin M.M. (1970) In: *Surface Area Determination* (D.H. Everett and R.H. Ottewill, eds) Butterworths, London, p. 123.
Dubinin M.M. (1975) In: *Progress in Surface and Membrane Science* vol. 9 (D.A. Cadenhead, ed.) Academic Press, New York, p. 1.
Dubinin M.M. (1979) In: *Characterisation of Porous Solids* (S.J. Gregg, K.S.W. Sing and H.F. Stoeckli, eds) *Society of Chemical Industry*, London, p. 1.
Dubinin M.M. and Stoeckli H.F. (1980) *J. Colloid Interface Sci.* **75**, 34.
Everett D.H. and Powl, J.C. (1976) *J. Chem. Soc. Faraday Trans. I* **72**, 619.
Fernandez-Colinas J., Denoyel R., Grillet Y., Rouquerol F. and Rouquerol J. (1989) *Langmuir* **5**, 1205.
Gonzalez M.T., Rodriguez-Reinoso F., Garcia A.N., Marcilla A. (1997) *Carbon* **35**, 8.
Gregg S.J. and Langford J.F (1969) *Trans. Faraday Soc.* **65**, 1394.
Gregg S.J. and Sing K.S.W. (1976) In: *Surface and Colloid Science*, Vol 9 (E. Matijevic, ed.) Wiley, New York, p. 336.
Gubbins K.E. (1997) In: *Physical Adsorption: Experiment, Theory and Applications* (J. Fraissard and C.W. Conner, eds) Kluwer, Dordrecht, p. 65.
Hill T.L. (1952) *Adv. Catalysis IV* 236.
Horvath G. and Kawazoe K. (1983) *J. Chem. Eng. Japan* **16**, 470.
Horvath, G. and Suzuki, M. (1997), In: *Physical Adsorption: Experiment, Theory and Applications* (J. Fraissard and C.W. Conner, eds) Kluwer, Dordrecht, p. 133.
Kaganer M.G. (1959) *Zhur. Fiz. Khim.* **33**, 2202.
Kaneko, K. (1996), In: *Adsorption on New and Modified Inorganic Sorbents* (Dabrowski A. and V.A. Tertykh, eds) Elsevier, Amsterdam, p. 573.
Kaneko K., Cracknell R.F. and Nicholson D. (1994) *Langmuir*, **10**, 4606.
Kenny M.B., Sing K.S.W. and Theocharis C. (1993) In: *Proc. 4th Int. Conf. on Fundamentals of Adsorption* (M. Suzuki, ed.) Kodansha, Tokyo, p. 323.
Lastoskie C., Gubbins K.E. and Quirke N. (1993) *J. Phys. Chem.* **97**, 4786.
Lecloux A. and Pirard J.P. (1979), *J. Colloid Interface Sci.* **70**, 265.
Lippens, B.C. and de Boer, J.H. (1965) *J. Catalysis* **4**, 319.
Lopez-Ramon M.V., Jagiello J., Bandosz T.J. and Seaton N.A. (1997) *Langmuir* **13**, 4435.
Maglara E., Pullen A., Sullivan D., Conner W.C. (1997) *Langmuir* **10**, 11.
Martin-Martinez J.M., Rodriguez-Reinoso F., Molina-Sabio M. and McEnaney B. (1986) *Carbon* **24**, 255.
McEnaney B. and Mays T.J. (1991) In: *Characterization of Porous Solids II* (F. Rodriguez-Reinoso, J. Rouquerol, K.S.W. Sing and K.K. Unger, eds) Elsevier, Amsterdam, p. 477.
Mikhail R. Sh., Brunauer S. and Bodor E.E. (1968) *J. Colloid Interface Sci.* **26**, 45.
Nicholson D. (1996) *J. Chem. Soc., Faraday Trans* **92**, 1.
Nicholson D. (1997) In: *Physical Adsorption: Experiment, Theory and Applications* (J. Fraissard and C.W. Conner, eds) Kluwer, Dordrecht, p. 105.
Olivier J.P. (1995) *J. Porous Materials.* **2**, 9.
Rodriguez-Reinoso F., Molina Sabio M., Gonzalez M.T. (1997) *Langmuir* **13**, 8.
Rowlinson J.S. (1985) *Proc. Roy. Soc. A.* **402**, 67.
Saito A. and Foley H.C. (1991) *AIChEJ* **37**, 429.
Seaton N.A., Walton J.P.R.B. and Quirke N. (1989) *Carbon* **27**, 853.
Steele W.A. (1973) *Surface Sci.* **36**, 317.
Steele W.A. (1974) *The interaction of gases with solid surfaces*, Pergamon, Oxford, p. 14.
Steele W.A. and Bojan M. J. (1997) In: *Characterization of Porous Solids IV* (B. McEnaney, T.J. Mays, J. Rouquerol, F. Rodriguez-Reinoso, K.S.W. Sing and K.K. Unger, eds) The Royal Society of Chemistry, Cambridge, p. 49.

Stoeckli H.F. (1977) *J. Colloid Interface Sci.* **59**, 184.
Stoeckli F. (1993) *Adsorption Sci. Tech.* **10**, 3.
Stoeckli H.F. and Ballerini L. (1991) *Fuel* **70**, 557.
Stoeckli H.F. and Huguenin D. (1992) *J. Chem. Soc., Faraday Trans.* **88**(5), 737.
Stoeckli H.F., Houriet J.Ph., Perret A. and Huber U. (1979) In: *Characterisation of Porous Solids* (S.J. Gregg, K.S.W. Sing and H.F. Stoeckli, eds) *Society of Chemical Industry*, London, p. 31.
Stoeckli H.F., Centeno T.A., Fuertes A.B. and Muniz J. (1996) *Carbon* **34**, 10.
Venero A. F. and Chiou J. N. (1988) *M.R.S. Symp. Proc.* **111**, 235.
Walton J.P.R.B. and Quirke N. (1989) *Mol. Simul.* **2**, 361.